3D SEGMENTATION OF RODENT BRAIN STRUCTURES USING ACTIVE VOLUME MODEL WITH SHAPE PRIORS

Shaoting Zhang[1], *Junzhou Huang*[1], *Mustafa Uzunbas*[1], *Tian Shen*[2], *Foteini Delis*[3], *Xiaolei Huang*[2], *Nora Volkow*[3], *Panayotis Thanos*[3], *Dimitris Metaxas*[1]

[1] CBIM, Rutgers, The State University of New Jersey, Piscataway, NJ, USA
[2] Computer Science and Engineering Department, Lehigh University, PA, USA
[3] Behavior Neuropharmacology and Neuroimaging Lab, Brookhaven National Laboratory, NY, USA

ABSTRACT

Object boundary extraction is an important task in brain image analysis. Acquiring detailed 3D representations of the brain structures could improve the detection rate of diseases at earlier stages. Deformable model based segmentation methods have been widely used with considerable success. Recently, 3D Active Volume Model (AVM) was proposed, which incorporates both gradient and region information for robustness. However, the segmentation performance of this model depends on the position, size and shape of the initialization, especially for data with complex texture. Furthermore, there is no shape prior information integrated. In this paper, we present an approach combining AVM and Active Shape Model (ASM). Our method uses shape information from training data to constrain the deformation of AVM. Experiments have been made on the segmentation of complex structures of the rodent brain from MR images, and the proposed method performed better than the original AVM.

Index Terms— Segmentation, deformable models, Active Volume Model, Active Shape Model, Shape prior, rodent brain

1. INTRODUCTION

Diagnosis of neurological and phychiatric disorders is mostly based on behavioral observations and on data from neuroanatomical measures (MR, CT). Retrospective studies have shown that neurological disorders are associated with specific morphological changes of the brain, which could be used for the early or differential diagnosis of the disease [9]. In this study, we propose an approach that will provide fast and accurate 3D segmentation of brain regions based on MR images of the rodent brain. Rodents are often used as models of human disease not only because they frequently exhibit key features of abnormal neurological conditions [5] but also because they are a convenient starting point for novel studies.

Related works: Deformable model based segmentation methods have been widely used with considerable success. We review some relevant work using contour or mesh based shapes. Kass et al. proposed Snakes [7], which are energy-minimizing splines with smoothness constraints and influenced by image forces. Gradient Vector Flow (GVF) [12] is then proposed to increase the attraction range of the original Snakes. Depending solely on the image gradient information, however, these methods may be trapped by noise and spurious edges. Region analysis strategies [15] have been incorporated in Snake-like models to improve their robustness to noise. Huang et al. present a strategy aimed at integrating shape and appearance in a unified space, which is named as Metamorphs [6]. The model has not only boundary shape but also interior appearance, making it more robust in segmentation. Efforts have been made on the integration of interior appearance into 3D models. A volumetric deformable model, Active Volume Model (AVM) [11], is proposed. The AVM model's shape is represented by a simplex mesh and its volumetric interior carries the various visual appearance feature statistics. However, this online learning based model does not have any shape prior information. Thus it is relatively sensitive to the quality of initialization and image information. Another group of deformable models is level set based methods [8]. Region information has also been incorporated [4]. These approaches have been widely used in tubular structure and 3D cortex segmentation tasks since they are topologically free and can be easily used in any dimension. Statistical modeling approaches such as Active Shape Model (ASM) [3] or Active Appearance Model (AAM) [2] are also widely used and have been successfully applied in cardiac [14] and brain [1] segmentation. These methods may need a large amount of 3D training data, whose creation and maintenance can be difficult and time consuming in practice.

In this paper, we present an approach to combine the advantages of both AVM and ASM, i.e., use online learning based AVM to deform the 3D mesh from image information, and then use ASM shape constraint to refine this intermediate result, and repeat these two steps until convergence. AVM does not rely on any offline learning, so we do not need a large set of 3D training data. As a tradeoff, AVM is sometimes sensitive to image noise and intensity inhomogeneity.

Thus shape constraint from ASM is then applied to refine the intermediate segmentation result. We train the ASM model in our approach using a small number of training data since we only need a rough statistical model to help AVM out of local minima, and the overall approach is mostly data driven. By combining these two approaches, the proposed method is particularly useful when there are a limited number of training samples and large variations among the samples. It is applied to segment complex structures in rodent brains, such as the cerebellum and the striatum. Numerous experiments have been designed to evaluate this method.

2. METHODOLOGY

Image alignment: First all brain scans (images) are aligned to the same reference brain whose orientation corresponds to the Paxinos stereotaxic position [10]. Alignment is performed with rigid transformations (rotations and translations), thus after alignment the volume and shape of brain structures do not change. Then the brain structures are manually segmented by clinical experts. A 3D surface mesh, composed of around $1,000$ vertices, is created for each reconstructed structures in brains. The results from traditional marching cubes may contain many artifacts, thus all meshes are post-processed using isotropic remeshing and detail preserving smoothing tools[1]. To obtain the one-to-one correspondence for each vertex, we choose one specific mesh as the reference mesh and use a local deformation technique [13] to warp it into all other meshes. Thus all resulting meshes share the same connectivity and topology, and a mean shape can be calculated. From observation, the variance of the mass centroid of these meshes is small (the standard deviation is less than $0.3mm$). Thus given an aligned test image, it is reasonable to predict the centroid using the mean value.

Deformation module: The smoothed mean shape is used as an initialization. However, it may not be close to the boundary of the testing data because of the variance. Thus deformable models are still needed for accurate segmentation. In order to fit to the boundary of an object, the traditional AVM is driven by both a gradient based data term and a region data term which are derived from image information. The overall external energy function consists of two terms: the gradient term E_g and the region term E_R. The overall energy function is:

$$E = E_{int} + k_e \cdot E_{ext} = E_{int} + k_e \cdot (E_g + k_R \cdot E_R) \quad (1)$$

where k_R is a constant to balance the contributions of the two external energy terms. k_e is for the balance between internal (smoothness) and external forces.

The gradient data term can be defined using the gradient map, edge distance map, or a combination of both. Denote a gradient magnitude map or the distance transform of an edge map as F_g, the gradient data term is defined as:

$$E_g = \int_\Lambda F_g(\mathbf{x}) d\Lambda,\ F_g = D^2_{edge}\ or\ F_g = -\left|\nabla I\right|^2 \quad (2)$$

where Λ denotes the surface mesh, D_{edge} refers to the unsigned distance transform of the edge map, and ∇I represents the image gradient.

The region term encodes constraints for the AVMs model-interior appearance statistics. Considering a module using intensity statistics, the object region is predicted according to the current model-interior intensity distribution. Having both foreground object and background probabilities, we obtain a binary map that represents the predicted object region by applying the Bayesian Decision rule. Connected component analysis is then applied on the binary map to retrieve the connected component that overlaps the current model. This connected region is considered as the current ROI. Let us denote the signed distance transform of the current model's surface shape as Φ_Λ, and the signed distance transform of the ROI boundary shape as Φ_R, the region-based external energy term is defined using voxels within a narrow band around the model surface as:

$$E_R = \int_\Lambda \Phi_\Lambda(\mathbf{v}) \Phi_R(\mathbf{v}) d\Lambda \quad (3)$$

The multiplicative term provides two-way balloon forces that deform the model toward the predicted ROI boundary. This allows flexible model initializations either overlapping the object or inside the object. The mesh deformation is based on standard Finite Element Method (FEM) and solved efficiently in a linear system.

Shape refinement module: The above formulation may not be able to avoid the local minimum or keep a specific shape, especially when the texture of image is complex. Thus a shape refinement procedure is added in our method to constrain the deformation. This procedure is similar to the shape updating step in ASM. First all meshes are aligned using similarity transformation. Note that the alignment here is for shapes instead of images. Then their statistics is captured by principal component analysis (PCA). Given a intermediate segmentation result, it is first transformed to the mean shape, and then mapped into PCA space to update the pose and shape parameters. Thus we can guarantee that the shape only deforms into shapes consistent with the training data. This step can prevent over-segmentation and provide a shape constraint. We adopt the following steps to deform the proposed model toward matching the desired object boundary.

1. Manually segment a small number of training data.
2. Use PCA to capture statistics (mean and variance) of these 3D shapes.
3. Initialize the AVM, i.e., stiffness matrix and step size for FEM, and the gradient magnitude or edge map.

[1] http://www.openflipper.org/

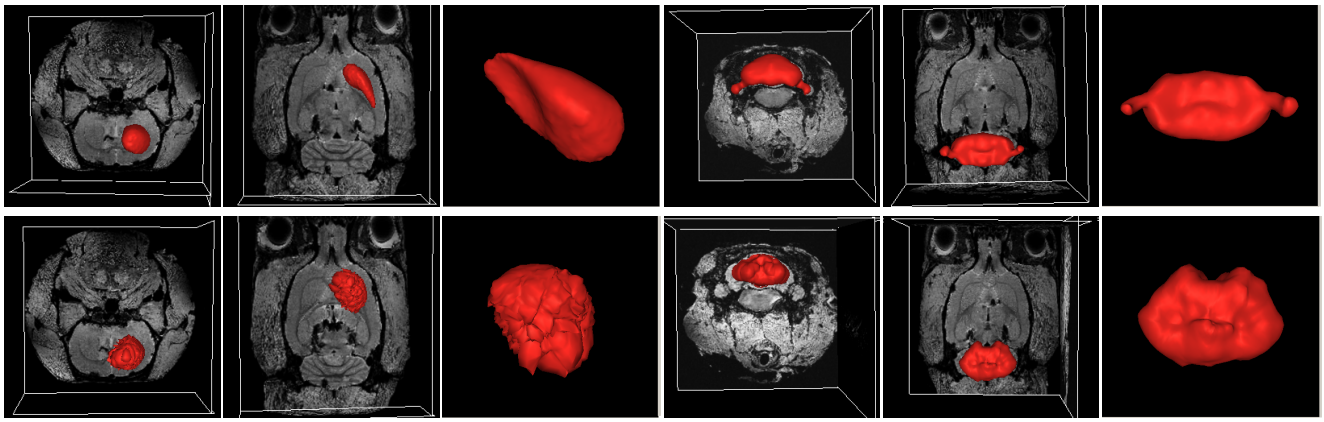

Fig. 1. Segmentation results of the striatum (the 1st to the 3rd column) and the cerebellum (the 4th to the 6th column) of the rodent brain. The 1st row: results from the proposed method. The 2nd row: results from AVM.

4. Compute Φ_Λ based on the current model; predict object ROI R by applying the Bayesian Decision rule to binarizing the estimated object probability map, and compute Φ_R. Calculate the external force vector.
5. Deform the model using FEM and external forces.
6. Refine this intermediate result by ASM shape constraint (transform it to the mean shape, then update the pose and shape parameters consistent with the training data).
7. Repeat steps 4-6 until convergence.

Alternatively employing the AVM deformation and the ASM shape refinement is more robust to noises and can handle more complex textures than purely using AVM. Our model converges fast and robust towards the boundary because of the benefit of the good-quality initialization and the constraint of the shape prior. One more benefit of our model is that the size of the training data can be small, because AVM is driven by current image information. Training information is only used for the shape refinement procedure, which is an auxiliary step in our model.

3. EXPERIMENTS

Experimental Settings: Adult male Sprague-Dawley rats were transcardially perfused with 4% paraformaldehyde. Heads were stored in paraformaldehyde and scanned for magnetic resonance imaging. The brains remained in the heads during scanning in order to avoid tissue and shape distortions during brain extraction. The heads were scanned on a 21.1T Bruker Biospin Avance scanner (Bruker Biospin Corporation, Massachusetts, USA). The protocol consisted of a 3D T2-weighted scan with echo-time (TE) $7.5ms$, repetition time (TR) $150ms$, 27.7 kHz bandwidth, field of view (FOV) of $3.4 \times 3.2 \times 3.0mm$, and voxel size $0.08mm$, isotropic. Out of 10 3D data, 7 were used as training to get mean mass centroid and other statistics, and the remaining 3 were used for testing. Both AVM and the proposed method were implemented in C++ and Python2.6 and tested on a 2.40 GHz Intel Core2 Quad computer with 8G RAM.

Table 1 compares the segmentation performance between our framework (including more sophisticated initialization and shape refinement) and the original AVM system. Cerebellum, left and right striatum of rodent brains are segmented. They are challenging for deformable models because of the relatively complex shapes and inside textures. The mean value of sensitivity (p), specificity (q), dice similarity coefficient (DSC) and relative errors of volume magnitude compared to ground truth are reported for evaluation. The number of iterations is also listed since the running time is proportional to it. Figure 1 shows the segmentation results of the methods with different view points in 3D. In the original AVM system, we manually place an ellipsoid and carefully rotate and resize it to an ideal position (close to the boundary) as the initialization, following the same procedure as the original paper [11]. Parameter tuning is in general a challenging problem for deformable models. We chose the parameter values in both models empirically. In the proposed method, shape constraints contribute to the stableness. Thus the result is less sensitive to parameter values.

Our proposed method achieves better quantitative performance and also better visual results. Its sensitivity, specificity and DSC are generally higher, while the number of iteration times for convergence are less. Note that all specificities are very high. The reason is that the segmented structures are relatively small, thus most background areas (true negatives) are successfully recognized.

Segmenting the left and the right striatum is challenging because the contrast between the structure and other surrounding brain structures is relative low. AVM can easily deform too much and over-segment the structure. Furthermore, with large smoothness energy (small k_e), AVM may fail to reach the sharp boundary of the striatum, while with large external energy (large k_e), AVM results may contain many small

Table 1. Quantitative evaluations and performance comparisons between AVM and the proposed method. RE-V denotes the relative error of estimated volume magnitude.

	AVM					Our method				
	p	q	DSC	#iterations	RE-V	p	q	DSC	#iterations	RE-V
Left striatum	0.75	0.98	0.62	28	1.138	0.82	0.99	0.89	7	0.084
Right striatum	0.70	0.99	0.61	32	1.025	0.81	0.99	0.84	8	0.129
Cerebellum	0.71	0.99	0.78	43	0.266	0.84	0.99	0.87	13	0.039

bumps because of the local intensity inhomogeneity and lack of smoothness constraints. The results can be observed in the second row of Figure 1. Using our method alleviates this problem since the ASM shape refinement step keeps the shape and prevents the over segmentation problem (the first row of Figure 1).

The cerebellum is also difficult to segment because of its complex internal textures and two protruding features. Its interleaving high gradient may make the model trapped in the local minimum. Large external force is needed to segment the protruding features, which adversely affects the smoothness of the model. Thus traditional AVM underperforms this task. Even though the quantitative results of AVM are reasonably good, we can clearly observe the artifacts from visual results. Our method uses ASM shape constraint to refine the intermediate result. The shape already escapes many local minima and it has two protruding features presented as priors. These properties not only improve the model's performance but also decrease the number of iterations to converge.

4. CONCLUSIONS AND FUTURE WORKS

In this work we proposed an algorithm to segment structures of the rodent brain. Based on a small set of training data, our method automatically places the initialization using the mean mass centroid and the smoothed mean shape, and also uses the shape information as a prior to constrain the deformation. It is more accurate and robust, and needs less iterations than AVM. Our method is more applicable when there is only a small number of training sampless. In the future, we would like to analyze and obtain statistics for more structures from more data. Furthermore, our current model can not handle structure missing. Efforts will be put on the modeling of these atypical situations. We are also interested in using the relative position and orientation among structures to facilitate the deformation.

5. REFERENCES

[1] K. Babalola, T. Cootes, C. Twining, V. Petrovic, and C. Taylor. 3D brain segmentation using active appearance models and local regressors. In *MICCAI*, pages 401–408, 2008.

[2] T. Cootes, G. Edwards, and C. Taylar. Active appearance models. *Proc. Of European Conf. on Computer Vision*, 2:484–498, 1998.

[3] T. Cootes, C. Taylor, D. Cooper, and J. Graham. Active shape model - their training and application. *CVIU*, 61:38–59, 1995.

[4] D. Cremers, M. Rousson, and R. Deriche. A review of statistical approaches to level set segmentation: Integrating color, texture, motion and shape. *IJCV*, 72(2):195–215, 2007.

[5] F. Delis, M. Xenos, D. Grandy, G.-J. Wang, and N. V. P. Thanos. Effects of chronic alcohol intake and dopamine D2 receptor gene expression on brain anatomy: an invivo MRI morphometric study of the mouse brain. In *Annual meeting of the Research Society on Alcoholism*, 2009.

[6] X. Huang, D. Metaxas, and T. Chen. Metamorphs: Deformable shape and texture models. In *CVPR*, pages 496–503, 2004.

[7] M. Kass, A. Witkin, and D. Terzopoulos. Snakes: Active contour models. *IJCV*, 1:321–331, 1987.

[8] R. Malladi, J. Sethian, and B. Vemuri. Shape modeling with front propagation: A level set approach. *PAMI*, 17:158–175, 1995.

[9] R. McCarley, C. Wiblea, M. Frumina, Y. Hirayasua, J. Levitta, I. Fischera, and M. Shenton. MRI anatomy of schizophrenia. *Biological Psychiatry*, 45(6):1099–1119, 2009.

[10] G. Paxinos and C. Watson. *The rat brain in stereotaxic coordinates*. Elsevier, Amsterdam, 2007.

[11] T. Shen, H. Li, Z. Qian, and X. Huang. Active volume models for 3D medical image segmentation. *CVPR*, 2009.

[12] C. Xu and J. Prince. Snakes, shapes and gradient vector flow. *TIP*, 7:359–369, 1998.

[13] S. Zhang, X. Wang, D. Metaxas, T. Chen, and L. Axel. LV surface reconstruction from sparse tMRI using laplacian surface deformation and optimization. In *ISBI*, 2009.

[14] Y. Zheng, A. Barbu, B. Georgescu, M. Scheuering, and D. Comaniciu. Four-chamber heart modeling and automatic segmentation for 3D cardiac ct volumes using marginal space learning and steerable features. *IEEE Trans. Med. Imaging*, 27:1668–1681, 2008.

[15] S. Zhu and A. Yuille. Region Competition: Unifying snakes, region growing, and Bayes/MDL for multi-band image segmentation. *PAMI*, 18(9):884–900, 1996.